Indian Journal of Fundamental and Applied Life Sciences ISSN: 2231– 6345 (Online)
An Open Access, Online International Journal Available at www.cibtech.org/sp.ed/jls/2015/02/jls.htm
2015 Vol. 5 (S2), pp. 3167-3179/Bahrami et al.

Research Article

SEISMIC PERFORMANCE EVALUATION OF WIDE-BODY AIRCRAFT HANGER

Alireza Bahrami, *Mazaher Rozbahani and Mehdi Alirezaei
Department of Civil Engineering, Malayer branch, Islamic Azad University, Malayer, Iran
**Author for Correspondence*

ABSTRACT
To accommodate wide-body aircrafts and creation of their maintenance areas, the area with dimension of 90 meters (from each side) is required. To cover an area having this range of width, often the customary designing is not efficient and to reach to such an areas, likely, hanger with costly and massive structure is needed. In designing of this type of structures the location of construction of the structure is one of the most important determinant factors of the type of designing. Iran is a seismic country, which is located on one of the big seismic belts of the world called as "Alpine-Himalayan", and occasionally large earthquakes occur. According to this significant issue, the performance of these type of massive structures against the forces due to earthquake should be evaluated. The aims of this research are: the seismic performance and behavior of a hanger having a large span under the lateral and normal forces, the relation of frame span and the effect of normal force of earthquake, nonlinear static analysis and nonlinear time history analysis of structure. In this research patterns with three different span and two heights are considered, and also for modeling of structure the SAP2000 software version 17 edition is used. Three types of accelerograms (Centro, 1979; Northridge, 1994, San Fernando 1971) for seismic performance evaluation are used.

Keyworlds: *Seismic Performance, Aircraft Hangers, Shed With Large Span, Seismic Design, Accelerograms, Nonlinear Static Analysis, Nonlinear Time History Analysis*

INTRODUCTION
Shed is a steel building with sloping roof which is designed and constructed on the basis of specific technical computing. This type of structure is used in construction of factories, buildings structure, storehouses, aviculture, aircraft hangers, workshops, shops and sportarenas, in which frames with large apertures are required. Due to enlargement of dimension of beams and columns, beam-plate should be used in shed profile.

The roof mechanism includes of bearing structure, a structural coverage and thermal and humidity insulation. The bearing structure of the roof consists of beam ortruss in each frame which is support of rafters of roof coverage (Affairs Office of Technical, 2006).

Truss is a rigid structure created by triangular units which are made of long and thin components. Trusses can just tolerate compressive and tensile forces. Trusses are one of the simplest bearing components of the structure which are operate as a bending component and they are used in roofs, bridges, and aerospace structures. In this type of structures, due to lack of exist of shear force and bending moment in each element, hinges should be modeled in hinge form. According to the definition, a truss creates by a set of elements which all are in one plane and their combination creates a triangular lattice. Assume each element from its ends is hinged to the other elements, therefore, this triangular form is the only stable form (Leylabadi, 2005).

Review of Previous Literature
In 1998, Kazakevitch in his article with the title of "aerodynamic roof membrane of aircraft hangers" has shown according to his experiments on various models, with increasing of aerodynamic of membrane roof, the upward lifting effect of wind force reduces, and by using this effect smaller units can be used. For this experiment he used the wind tunnel which at that time this tunnel was used for aircraft and car experimentations. He used three models of simple, Semi-aerodynamic and full-aerodynamic. The full-aerodynamic model was in the shape of curved roof (Kazakevitch, 1998).

Luke and Howson (2002) in their article with the title of "Modern aircraft hangers: A review of design trends and requirements" publishing in 2002 studied about common design method of hangers and the loading combinations and regulations, and also they offered an optimum method and flowchart to design on the basis of span length and the type of structural system. This article mentions to various hanger shapes and various proposed materials for a modern hanger. For the roof of these structures also truss system and cable system are recommended. Further, according to structural performance and length to width ratio, the plan of some hangers existing in Iceland, Russia, England and US are evaluated and concludes the plans having symmetrical geometry and rigidity have more appropriate behavior. This article also mentions the problems and issues of symmetrical plans, and for construction of several resembling hangers, recommends they should design next to each other considering require separation distance and using cable roof.

Qian *et al.,* (2008) in their article with the title of "Application of pushover analysis on earthquake response prediction of complex large-span steel structure" publishing in 2008, specifically concentrate on truss structures in large span. This article by analyzing the A380 hanger located in Beijing and the football stadium of this city as two large span truss structures, evaluates their earthquake responses. For earthquake response analysis, they evaluated 12 different types of lateral loading under earthquake response analysis. They compared the observations of this pushover analysis to the observation of nonlinear time history analysis. As a result, in pushover analysis for steel truss structures on large spans, according to obtained graphs, the modal mass participation factor for these structures is higher than 0.65 and there for pushover analysis observations will closer to dynamic analysis observations. According to this research it seems pushover analysis can accurately predict steel structure response with large span to the sever earthquakes.

Research Aims

The aims of this research are: seismic performance and seismic behavior of a large span hanger under lateral and normal forces, relation of frames span and effect of earthquake normal force, execution of nonlinear static analysis and nonlinear time history analysis of structure.

MATERIALS AND METHODS

To reachtoseismic correct performance of a structure, the accessible resistance and deformation capacity of elements should not be more than imposed requirements on the structure by the earthquake. According to the behavior of structure at the earthquake time, its accurate performance evaluation should be performed by nonlinear time history analysis using selected earthquakes. By entrance of the structure into the gamut of nonlinear behavior under earthquake effect, movements give a better explanation of the structure response with respect to forces, and by restricting displacements instead of forces, the level of destruction of the structure effectively can be controlled.

Changing the viewpoint from designing on the basis of force to designing on the basis of behavior and performance of structure offers a new method of design called as designing on the basis of performance (Performance Base Seismic Design). Designing on the basis of performance is on the basis of designing in limitation conditions. To access to the structure capacity on the other side of elastic range, using the nonlinear analysis is needed. Estimation of seismic requirements in low performance level such as safety of life and prevention of all structures destruction requires vast consideration in inelastic performance of the structure (Asghari, 2010).

1) Nonlinear Time History Analysis, RHA

Nonlinear time history analysis is one of the nonlinear dynamic analysis methods, it is complicated and nevertheless the most accurate method to evaluate structure inelastic requirements under accelerograms effect of earth movement. To determine probable performance of the structure under a specific earthquake, the observation of this analysis can directly compare to observed data from experiments executed on the structural components samples. In time historical analysis, due to structure softening during the earthquake, the higher modes effects and changes in interia load pattern are considered automatically. In this method, maximum total displacement which is applied to structure by a specific

Indian Journal of Fundamental and Applied Life Sciences ISSN: 2231– 6345 (Online)
An Open Access, Online International Journal Available at www.cibtech.org/sp.ed/jls/2015/02/jls.htm
2015 Vol. 5 (S2), pp. 3167-3179/Bahrami et al.

accelerogram, is directly determined and estimation of this parameter on the basis of theoretical-experimental relations is not required.

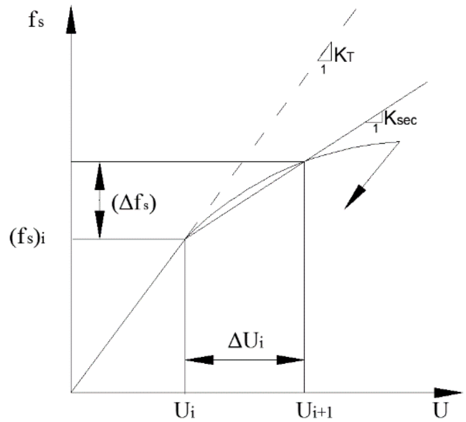

Figure 1: Structure behavior diagram

2) Accelerogram

As our selected structure in land type III (3) is conforming to standard 2800 of Iran, accelerograms accelerations also should be selected from the same considering soil i.e. type III.

Based on given article by Niknam and Eskandari (2010) with title of "Performance evaluation of concrete moment frame system using produced accelerograms acceleration", soils type C and D of bottom table are equivalent to soils type III and IV of Iran standard 2800.

No	Event	Station	ϕ° [1]	Soil[2]	M[3]	R[4] (km)	PGA (g)
1	Northridge, 1994	LA, Baldwin Hills	090	B,B	6.7	31.3	0.239
2	Imperial Valley, 1979	Compuertas	285	C,D	6.5	32.6	0.147
3	Imperial Valley, 1979	Plaster City	135	C,D	6.5	31.7	0.057
4	Loma Prieta, 1989	Hollister Diff. Array	255	–,D	6.9	25.8	0.279
5	San Fernando, 1971	LA, Hollywood Stor. Lot	180	C,D	6.6	21.2	0.174
6	Loma Prieta, 1989	Coyote Lake Dam Downstream	285	B,D	6.9	22.3	0.179
7	Imperial Valley, 1979	Cucapah	085	C,D	6.5	23.6	0.309
8	Northridge, 1994	LA, Hollywood Storage FF	360	C,D	6.7	25.5	0.358
9	Loma Prieta, 1989	Anderson Dam Downstream	360	B,D	6.9	21.4	0.24
10	Loma Prieta, 1989	Hollister South & Pine	000	–,D	6.9	28.8	0.371
11	Loma Prieta, 1989	Sunnyvale Colton Ave	360	C,D	6.9	28.8	0.209
12	Superstition Hills, 1987	Wildlife Liquefaction Array	090	C,D	6.7	24.4	0.18
13	Imperial Valley, 1979	Chihuahua	282	C,D	6.5	28.7	0.254
14	Imperial Valley, 1979	El Centro Array #13	230	C,D	6.5	21.9	0.139
15	Imperial Valley, 1979	Westmoreland Fire Station	180	C,D	6.5	15.1	0.11
16	Loma Prieta, 1989	Halls Valley	090	C,C	6.9	31.6	0.103
17	Superstition Hills, 1987	Wildlife Liquefaction Array	360	C,D	6.7	24.4	0.2
18	Imperial Valley, 1979	Compuertas	015	C,D	6.5	32.6	0.186
19	Imperial Valley, 1979	Plaster City	045	C,D	6.5	31.7	0.042
20	San Fernando, 1971	LA, Hollywood Stor. Lot	090	C,D	6.6	21.2	0.21

[1] Component [2] USGS, Geomatrix soil class [3] moment magnitude [4]closest distance to fault rupture

Figure 2: Existing Accelerograms

Based on this table we use accelerograms number 8 (Northridge, 1994), number 14 (El Centro, 1979) and number 20 (San Fernando, 1971) which are in soils type C and D or soil type III. Their rate of PGA are in the order of 0.358, 0.139, 0.21. to make the accelerograms tantamount they should multiply by their invers PGA. For this, the seismosignal (Free download In site : www.seismosoft.com) software is used.

Response spectrums of each accelerogram pair combine to each other using the method of square root of thesum of squares (SRSS) and one unit-combined spectrum for each pair produces.

3) Review Models Introduction

In this research as a model, a type of shed having roof system of two-truss lattice is considered, which lower truss lattice is flat form and upper one is curved form. These models includes two elevation types of 10 and 20 meters and three span types of 30, 60, 90 meters. For truss elements section, pipe section is used and also for columns, wide wing section is used.

4) Static Loading Of Model

Roof dead load (coverage, insulation, steel elements) 50 Kg/m^2
Roof imposed load 100 Kg/m^2
Snow imposed load 150 Kg/m^2
To exert of wind load, Canada regulation NBCC (National Building Code of CANADA) is used
To exert of earthquake force in the structure and its distribution, the UBS97 (Uniform Building Code 1997) regulation is used.

5) Load Combination

In this article following load combinations are used which are according to journal number 325 of management and planning organization of Iran (Affairs, Office of Technical, 2006).

1) DL
2) DL+LL+SL
3) DL+WL
4) DL+EL
5) DL+LL+(0.5SL)+WL
6) DL+LL+(0.5SL)+EL
7) DL+LL+SL+(0.5WL)
8) DL+LL+SL+(EL)

In this research for more accuracy the direct integration method which is relatively long term method is used and this analysis should perform exactly after nonlinear static analysis with coefficient of 1.1(DL+LL). After introduction of all the parameters related to modeling, evaluation is performed and the observation will be reviewed.

RESULTS AND DISCUSSION

Following observations are obtained from the node in the middle of the model span in the low part of truss:

Table 1: observation from the node in the middle of model span in low part of truss

Model		**Displacement in meters**						
Height	**Width**	**DL**	**LL**	**Snow load**	**Wind load**	**Combo no.3**	**Combo no 4.1**	**Combo 5.1**
10 meter	**30 m**	-0.047	-0.083	-0.12	0.05	-0.047	-0.19	-0.25
	60 m	-0.28	-0.46	-0.7	0.29	-0.28	-1.1	-1.45
	90 m	-1.54	-2.12	-3.19	0.29	-1.54	-5.21	-6.86
20 meter	**30 m**	0.047	-0.083	-0.12	0.85	0.09	-0.19	-0.25
	60 m	-0.28	-0.46	-0.7	4.55	0.55	-1.1	-1.46
	90 m	-1.54	-2.12	-3.19	4.82	-1.54	-5.27	-6.78

Indian Journal of Fundamental and Applied Life Sciences ISSN: 2231– 6345 (Online)
An Open Access, Online International Journal Available at www.cibtech.org/sp.ed/jls/2015/02/jls.htm
2015 Vol. 5 (S2), pp. 3167-3179/Bahrami et al.
Research Article

Plastic hinges deformation under horizontal accelerograms:

Table 2: Plastic hinges deformation under horizontal accelerograms

		El Centro		**Northridge**		**San Fernando**	
Height	**Width**	**Force**	**Displacement**	**Force**	**Displacement**	**Force**	**Displacement**
10 m	20 m	44142.05	0.06387	278199.71	0.00034	277631.05	0.00016
		-275994.72	-0.0004	44181.42	0.063	303155.57	0.0082
		40980.83	-0.0034	-26324.89	-0.00047	-14713.33	-0.0138
		-23595.58	-0.0053	27597.12	0.000788	-26059.07	0.0021
	60 m	-373718	-0.00496	14113.08	0.00	16855.81	0.00
		-393770	-0.00298	10497.06	0.00	16855.81	0.00
		3667.41	-0.033	23110.42	-0.033	-9006.76	-0.0036
		-9343.26	-0.002	-9634.89	-0.0007	-8723.74	-0.000688
	90 m	22004.79	-0.033	101973.11	0.00799	-849564.98	-0.00052
		-9303.97	-0.0024	227409.58	0.000217	153232.02	0.0958
		-9549.04	-0.0008	9584.73	-0.00042	-9614	-0.000611
		3610.54	0.00	-7757.35	-0.00882	-9359.54	-0.00018
20 m	20 m	280309.81	0.001	157637.06	-0.00073	136768.78	0.00
		288371.82	0.0035	44225.61	0.063	73586.38	0.00
		-27082.92	-0.002	12068.31	-0.0277	-16781.36	-0.000953
		23500.17	0.042	40980.77	-0.000868	28326.37	0.00019
	60 m	445036.19	0.0018	-401827.58	-0.0021	509551.05	0.05003
		-297908.94	-0.0022	164289.33	0.000748	56817.39	-0.000314
		-9474.77	-0.0017	-7802.51	-0.00090	7066.1	-0.000314
		4609.29	-0.033	21798.38	0.0102	-9648.95	-0.000838
	90 m	1219845.34	0.045	-825272.2	0.000054	697101.96	0.00
		857992.52	-0.0017	67489.32	-0.000088	702569.16	0.00
		-8625.01	-0.005	-7362.79	-0.0104	-9573.76	-0.00129
		19989.8	0.0021	-2912.23	0.0199	-9144.05	-0.00307

Plastic hingedeformation under vertical accelerograms:

Table 3: Plastic hinges deformation under vertical accelerograms

		El Centro		**Northridge**		**San Fernando**	
Height	**Width**	**Force**	**Displacement**	**Force**	**Displacement**	**Force**	**Displacement**
10 m	**20 m**	26409.4	-0.00091	64430.26	-0.000353	-277666.03	0.00107
		-252595.12	-0.027	-243257.84	-0.0279	284738.58	0.00241
		-27964.26	-0.0075	35294.08	0.00823	10797.14	0.00838
		-25870.81	-0.00314	-21307.04	-0.0075	-27717.52	-0.000099
	60 m	545753.02	0.032	-31414.83	0.00	-11042.81	0.00
		545927.53	0.032	-27985.5	0.00	-20362.87	0.00
		-9611.57	-0.0052	-9314.66	-0.0023	-9589.22	-0.00045
		-9611.63	-0.0052	-8002.97	-0.000033	-9532.71	-0.000083
	90 m	-849306.14	-0.00048	-397077.82	-0.000023	-300208.69	0.00
		1055217.8	0.052	-345985.04	-0.000017	471496.67	0.00
		-5616.07	0.011	-6639.88	-0.000873	-9599.82	-0.00118
		-9586.2	-0.0012	-9570.3	-0.000327	-8686.27	-0.0044
20 m	**20 m**	44336.06	0.063	44336.06	0.0638	143501.8	0.000437
		170533.56	0.007	87217.4	0.0149	310781.24	0.0106
		26599.63	-0.0064	43339.5	0.0288	-19313.49	-0.0094
		-19686.38	0.0034	32955.19	0.000967	18206.46	-0.00082
	60 m	565852.91	0.038	-322634.66	-0.0418	71763.75	0.00
		565853.19	0.038	148510.59	0.00	198316.83	0.000044
		21731.68	0.00977	-7443.65	-0.0101	9727.66	-0.033
		21731.66	0.00977	20303.24	-0.033	-9556.91	-0.00024
	90 m	974438.03	0.0022	889046.47	0.00	-183729.7	0.00
		-850457.76	-0.000646	-115854.6	0.00	-181115.5	0.00
		-9270.06	-0.0000068	-8437.48	-0.006	-9398.34	-0.002
		20296.85	0.0044	8083.53	0.00	7714.71	0.00

Indian Journal of Fundamental and Applied Life Sciences ISSN: 2231– 6345 (Online)
An Open Access, Online International Journal Available at www.cibtech.org/sp.ed/jls/2015/02/jls.htm
2015 Vol. 5 (S2), pp. 3167-3179/Bahrami et al.
Research Article

Dynamic base shear under horizontal accelerograms:

Table 4: Dynamic base shear under horizontal accelerograms

			El Centro		**Northridge**		**San Fernando**	
Height	**Width**	**Base Shear**	**Force**	**Period**	**Force**	**Period**	**Force**	**Period**
10 m	**20 m**	Min in X direction	-1.485E04	4.050E-01	-1.410E04	4.600E-01	-9.849E03	4.300E-01
		Max in X direction	1.414E04	3.30E-01	1.962E01	2.600E-01	7.336E03	3.500E-01
		Min in Z direction	-8.49E04	3.850E-01	-5310E04	5.000E-01	-2.238E05	3.900E-01
		Max in Z direction	-9.281E04	3.900E-01	3.703E04	0.00	1.494E05	3.700E-01
	60 m	Min in X direction	-5.781E01	2.650E-01	1.764E07	0.00	1.321E03	3.900E-01
		Max in X direction	1.401E05	4.950E-01	5.313E02	3.600E-01	3.552E02	3.200E-01
		Min in Z direction	-2.172E05	4.950E-01	-2.174E04	3.000E-01	-1.743E04	3.500E-01
		Max in Z direction	1.721E05	5.050E-01	1.286E04	2.200E-01	1.481E04	3.500E-01
	90 m	Min in X direction	-2.773E00	5.00E-03	-5.820E03	1.020E00	-1.849E04	5.600E-01
		Max in X direction	2.649E02	4.050E-01	2.495E05	1.040E00	2.827E01	3.600E-01
		Min in Z direction	-1.879E04	3.100E-01	-7.765E05	1040E00	-4.201E04	5.300E-01
		Max in Z direction	2.123E05	3.800E-01	2.625E05	1.020E00	4.024E04	5.500E-01
20 m	**20 m**	Min in X direction	-9.375E02	3.200E-01	-2.071E00	2.200E-01	-2.989E03	4.700E-01
		Max in X direction	9.287E02	3.750E-01	4.468E03	5.000E-01	2.180E01	1.900E-01
		Min in Z direction	-7.128E04	3.750E-01	-7.971E04	5.000E-01	-1.082E05	4.700E-01
		Max in Z direction	6.418E04	3.650E-01	3.798E04	0.00	8.328E04	4.200E-01
	60 m	Min in X direction	-8.059E03	5.100E-01	-7.745E-01	1.600E-01	-5.344E03	4.800E-01
		Max in X direction	2.495E02	4.250E-01	1.550E04	5.600E-01	1.949E01	3.500E-01
		Min in Z direction	-1.167E05	5.50E-01	-3.974E04	5.600E-01	-5.540E04	4.800E-01
		Max in Z direction	6.373E04	4.250E-01	1.258E04	0.00	3.502E04	3.700E-01
	90 m	Min in X direction	-5.538E00	5.000E-03	-3.734E-02	9.400E-01	-3.732E02	5.500E-01
		Max in X direction	4.459E03	5.500E-01	2.448E02	9.800E-01	2.780E01	3.600E-01
		Min in Z direction	-2.112E04	5.500E-01	-2.772E04	9.400E-01	-1.375E04	5.200E-01
		Max in Z direction	2.065E4	4.400E-01	2.651E04	1.000E00	1.813E04	4.500E-01

Dynamic base shear under vertical accelerograms:

Table 5: Dynamic base shear under vertical accelerograms

			El Centro		**Northridge**		**San Fernando**	
Height	**Width**	**Base Shear**	**Force**	**Period**	**Force**	**Period**	**Force**	**Period**
10 m	20 m	Min in X direction	-3.030E02	2.050E-01	3.751E04	4.200E-01	-2.963E04	4.100E-01
		Max in X direction	2.090E04	4.100E-01	6.276E02	3.200E-01	3.990E03	3.100E-01
		Min in Z direction	-6.050E04	4.100E-01	-5.262E04	4.200E-01	-6.296E04	3.800E-01
		Max in Z direction	4.918E04	4.050E-01	3.703E04	0.00	3.703E04	0.00
	60 m	Min in X direction	-6.364E01	4.200E-01	-8.831E00	2.400E-01	-2.476E01	1.600E-01
		Max in X direction	2.161E-03	1.700E-01	1.020E02	3.400E-01	2.129E02	2.800E-01
		Min in Z direction	-4.979E04	4.200E-01	-1.550E04	2.200E-01	-2.244E04	2.800E-01
		Max in Z direction	-3.919E04	2.100E-01	2.729E04	2.600E-01	2.136E04	2.300E-01
	90 m	Min in X direction	-1.214E04	4.400E-01	-1.786E02	6.600E-01	-2.773E00	5.000E-01
		Max in X direction	2.284E01	2.750E-01	1.479E04	7.600E-01	6.244E03	6.500E-01
		Min in Z direction	-2.941E04	4.250E-01	-4.127E04	7.600E-01	-4.690E04	5.750E-01
		Max in Z direction	2.683E04	3.450E-01	1.664E04	6.600E-01	2.413E04	6.800E-01
20 m	20 m	Min in X direction	-4.624E02	2.950E-01	-3.627E02	4.200E-01	-2.238E01	1.200E-01
		Max in X direction	1.967E03	3.850E-01	3.019E03	5.000E-01	3.750E03	4.300E-01
		Min in Z direction	-6.975E04	3.700E-01	-1.547E05	5.000E-01	-6.379E04	4.300E-01
		Max in Z direction	6.989E04	3.600E-01	2.090E05	5.200E-01	4.779E03	4.200E-01
	60 m	Min in X direction	-4.269E01	5.100E-01	-2.425E03	5.600E-01	-4.554E03	4.900E-01
		Max in X direction	3.174E01	5.000E-01	2.909E03	5.000E-01	3.467E01	2.600E-01
		Min in Z direction	-8.418E04	4.900E-01	-3.900E04	4.400E-01	-4.418E04	4.900E-01
		Max in Z direction	9.136E04	4.800E-01	6.314E04	5.400E-01	3.528E04	3.600E-01
	90 m	Min in X direction	-3.326E00	4.400E-01	-3.020E01	8.000E-01	-1.577E02	4.400E-01
		Max in X direction	1.751E03	6.400E-01	9.547E02	1.040E00	2.154E02	6.200E-01
		Min in Z direction	-1.424E04	6.300E-01	-1.803E04	8.000E-01	-1.321E04	5.200E-01
		Max in Z direction	1.381E04	6.00E-01	1.302E04	1.000E-01	1.675E04	3.900E-01

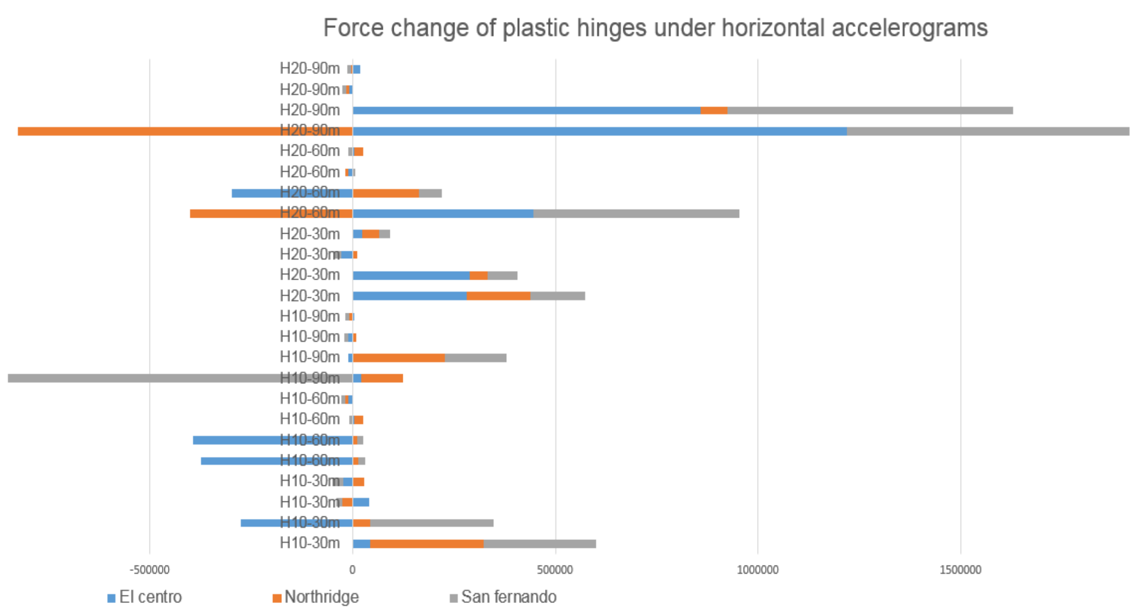

Figure 3: Force change diagram of plastic hinges under horizontal accelerograms

According to the above diagram, the maximum force in horizontal acceleration of El- Centro applies to the structure.

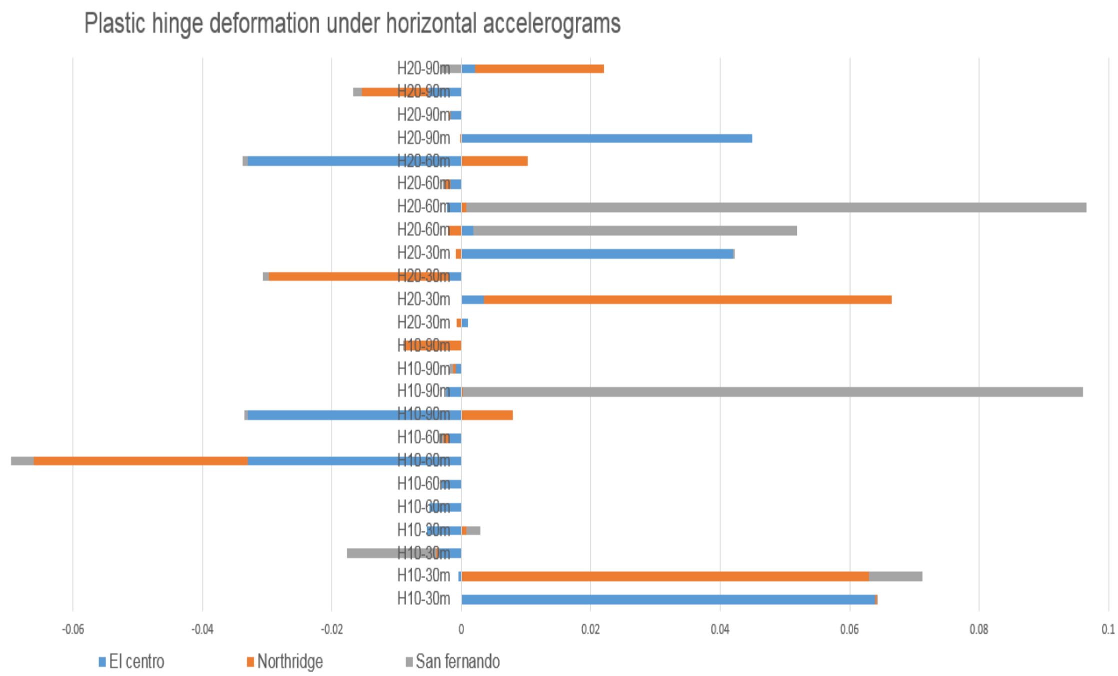

Figure 4: Diagram of plastic hinge deformation under horizontal accelerograms

According to the above diagram, the maximum plastic deformation in horizontal acceleration of Northridge appears in the structure.

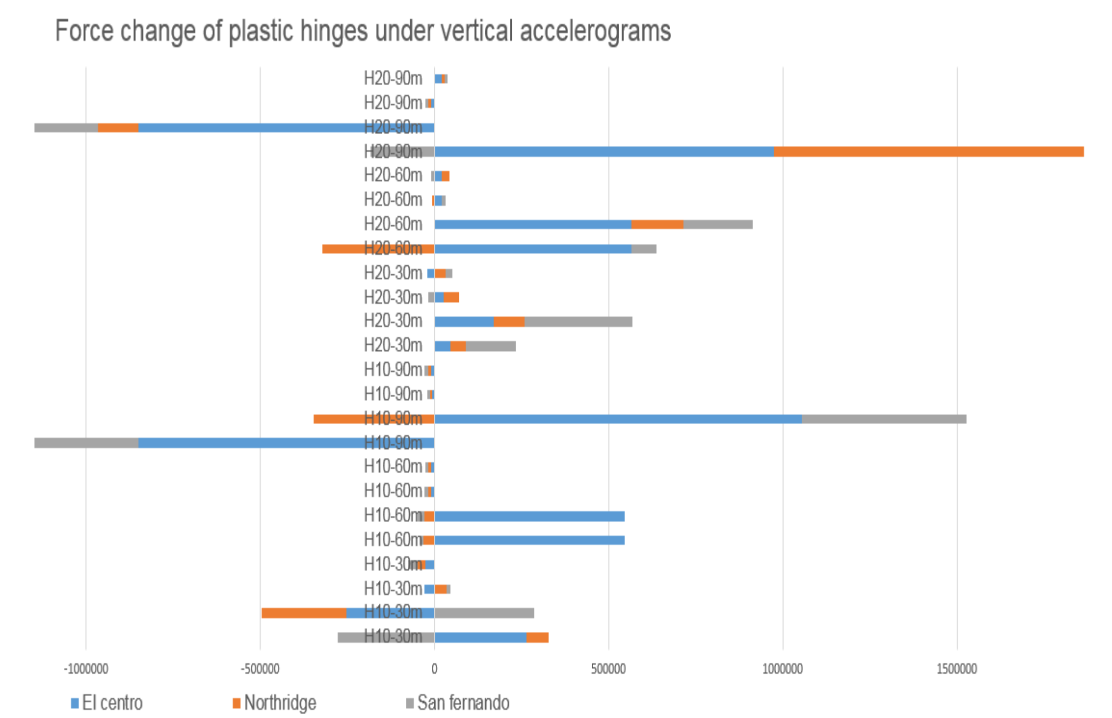

Figure 5: Force change diagram of plastic hinges under vertical accelerograms

According to the above diagram, the maximum force in vertical acceleration of El Centro applies to the structure.

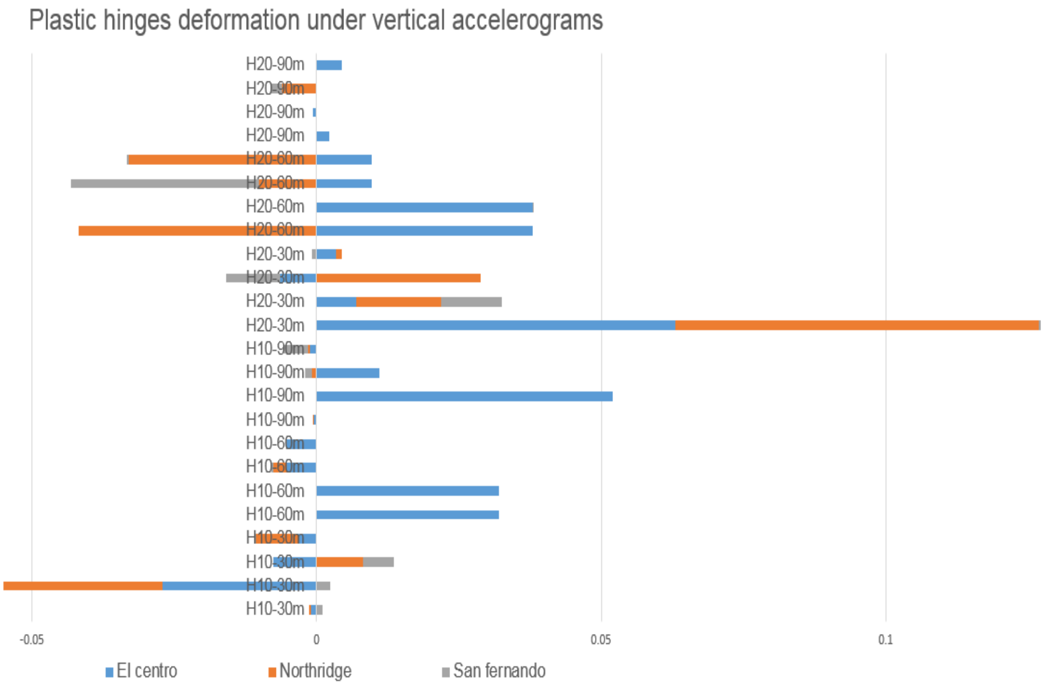

Figure 6: Diagram of plastic hinges deformation under vertical accelerograms

According to the above diagram, the maximum plastic deformation in horizontal acceleration of El Centro and Northridge appears in the structure.

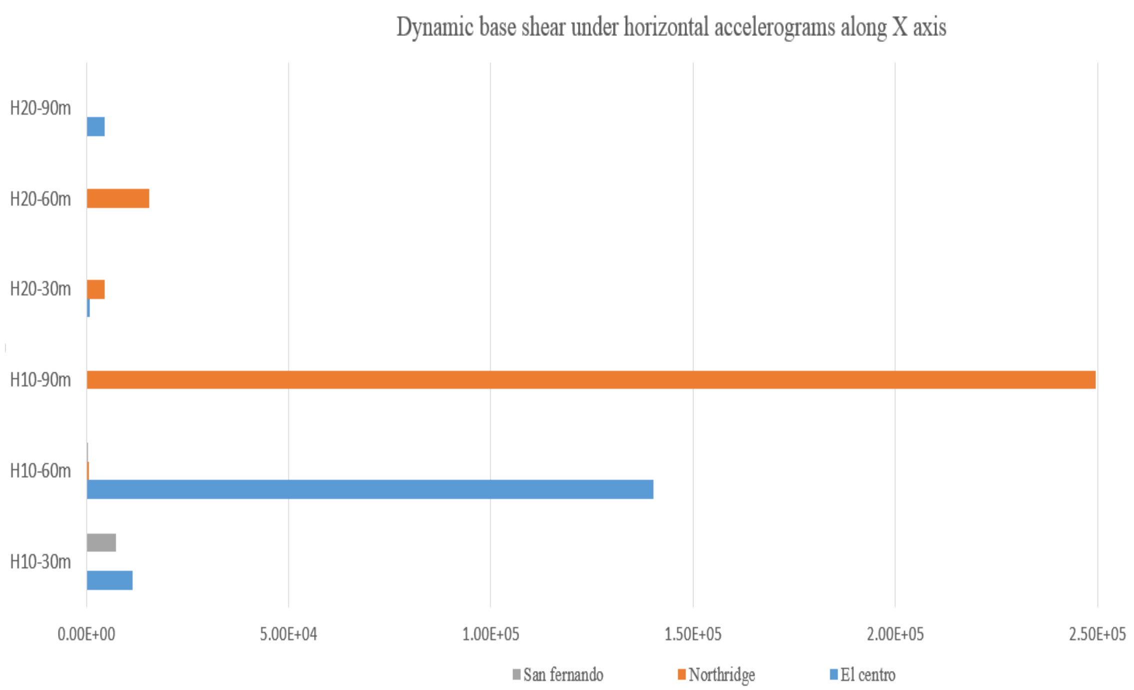

Figure 7: Diagram of dynamic base shear under horizontal accelerograms along X-axis

According to the above diagram, the maximum dynamic base shear along X-axis also produces in horizontal acceleration state of Northridge in span of 90 meters.

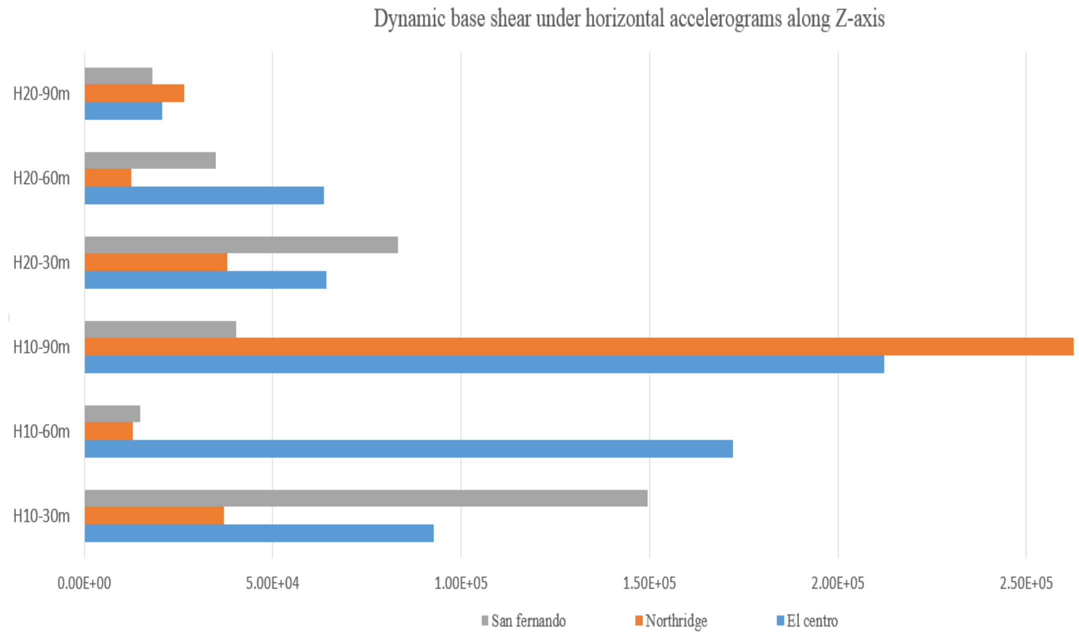

Figure 8: Diagram of dynamic base shear under horizontal accelerograms along Z-axis

According to the above diagram, the maximum dynamic base shear along Z-axis also produces in horizontal acceleration state of Northridge in span of 90 meters. Consider, in the majority of models the maximum rate of base shear is under horizontal acceleration of San Fernando, but in the case of total maximum rate, horizontal acceleration of Northridge is considered.

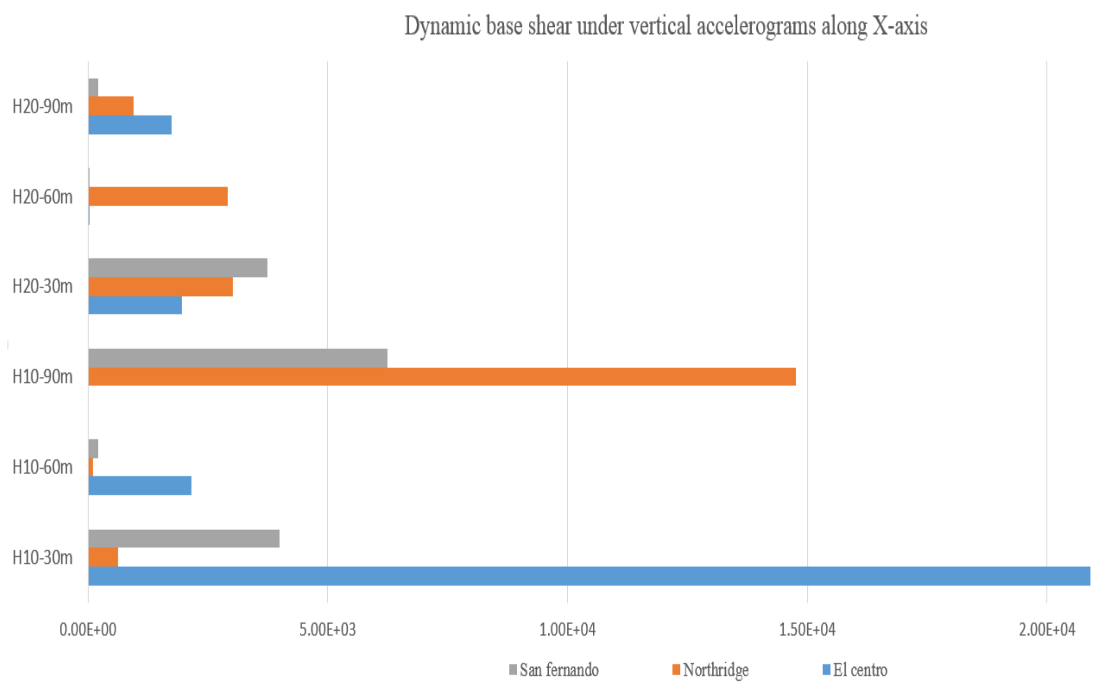

Figure 9: Diagram of dynamic base shear under vertical accelerograms along X-axis

According to the above diagram, the maximum dynamic base shear along X-axis also appears in vertical acceleration state of El Centro.

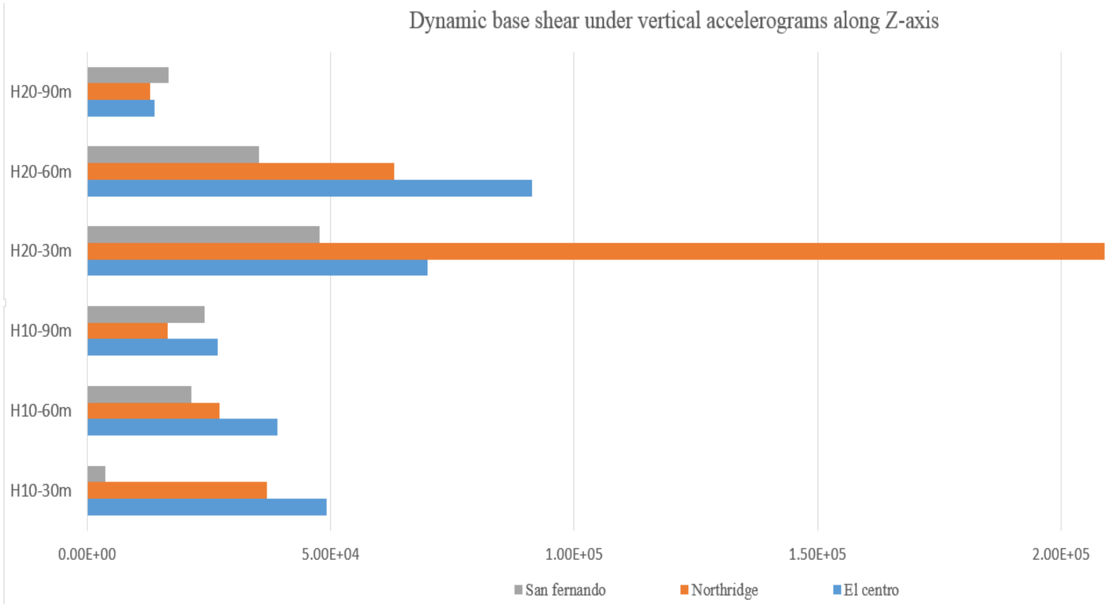

Figure 10: Diagram of dynamic base shear under vertical accelerograms along Z-axis

Discussion

1. According to the obtained observations truss elements deformation in large span significantly increases, therefore for the span of higher than 60 meters using thethree dimensional truss or space frames is recommended.

2. Lower section of truss performs in bending form and therefor to tolerate of these forces, higher moment of interia in the middle of span is required. Then the section of low truss is recommended to build in the form of beam-plate with changeable section similar to shed beams, but the cross section in the middle of span is bigger than the edges.

3. With increase in number of truss lattices, force distribution is better, therefore, for the spans of larger than 60 meters, increasing in the number of truss lattices is recommended.

4. Remember, increasing the number of truss lattices increases the weight of roof, to solve of this issue, evaluation of optimum ratio for this case is recommended.

5. While the pipe sections are used for truss elements, plastic hinges produce regularly in the structure and depreciate forces more effectively.

6. During the evaluations, the wind force is less effective than earthquakeforce, therefore, while the figure and dimension of the structure is in this form, for the future evaluation these force displacements can be dismissed.

7. With linear and nonlinear static states evaluation we realize with creation of plastic hinges and nonlinear state of materials, the entire of their maximum load capacity is used and the other sections which do not fall in the nonlinear phase can be reduced. This scheme reduces the structure weight andsubsequently according to second law of Newton the effect of acceleration factors reduces.

8. In models having span until 60 meters, changes due to vertical factors of earthquake almost are less than horizontal factors of earthquake, but when the span becomes larges than this rate, these changes increase significantly and become one of the effective factors of designing.

9. The changes in elevation from 10 to 20 meters in small spans do not make any impressive change in the results, of course in spans of larger than 60 meters, those are effective on structure response proceeding.

10. According to dynamic base shear analysis in the state of horizontal accelerograms we realize in large span this section increases increasingly. Then, in foundation and column base designing, this effect should be applied and in the foundation specific schemes such as preparation of shear key of foundation.

11. According to dynamic base shear in vertical accelerograms state, we realize the rate of changes is high and quick reciprocal movements occur, therefore, the type of hinges and their resistance to tolerate these quick cycles is important.
12. In dynamic base shear under horizontal accelerograms along X axis, accelerations of Northridge and El Centro are in the highest rate so that the rate of San Fernando acceleration is not appreciable.
13. In dynamic base shear under horizontal accelerograms along Z axis, the accelerations of Northridge and El Centro are in the highest rate and in some states San Fernando acceleration will be more. The maximum rates are from accelerations of Northridge and El Centro.
14. In dynamic base shear under vertical accelerograms along X axis, the accelerations of El Centro and Northridge are in the highest rate and only in 30 meters span and 20 meters height state, San Fernando acceleration is more than the others.
15. In dynamic base shear under vertical accelerograms along Z axis, the accelerations of Northridge and El Centro are in the highest rate and only in 90 meters span and 20 meters height state San Fernando acceleration is more than them.

ACKNOWLEDGEMENT
We are grateful to Islamic Azad University, Malayer branch authorities, for their useful collaboration.

REFERENCES
Affairs Office of Technical. (2006). *Customer Design and Calculation of Steel Buildings,* Publication No. 325 (Tehran: Management and Planning organization).
Asghari Sorkhi M (2010). Introduction to the concepts of nonlinear analysis. *Bahonar University of Kerman* **14** 22-30.
Kazakevitch M (1998). The aerodynamics of a hangar membrane roof. *Journal of Wind Engineering* **78** 157-169.
Leylabadi A (2005). *Structural Analysis* (Tehran: publications SID unit Amir Kabir).
Niknam A and Eskandari M (2010). Performance evaluation of concrete moment frame system using produced accelerograms acceleration. *The Fifth National Congress on Civil Engineering, Ferdowsi University of Mashhad, Iran.*
Qian JR, Zhang WJ and Ji XD (12-17 October 2008). Application of pushover analysis on earthquake response. *The 14 th World Conference on Earthquake Engineering, Beijing, China.*
Shayan S, Zaree G and Haghpanah Y (2013). Seismicity Iran. *Institute for Humanities and Cultural Studies,* **21.**
Steven J Luke and Paul W (2002). Modern aircraft hangars:. *The Institution of Structural Engineers USA, August*, 23-30.